IJESKA
contribution to science

www.ijeska.com
ISSN: 2687-5993
DOI:

International Journal of Earth Sciences Knowledge and Applications

RESEARCH ARTICLE

Petrogenesis of Heiran area submarine lavas in north east of Ardabil, Iran: A case study of Sevan-Akera-Qaradagh Ocean back arc basin

Yousef Vasigh[1]*, Erkan Aydar[2], Shahriyar Karimdoust[3], Ekrem Kalkan[3], Abdulvahab Mukhtarov[4]

[1]Islamic Azad University, Department of Geography, Ardabil Branch, Ardabil, Iran
[2]Hacettepe University, Engineering Faculty, Department of Geological Engineering, Ankara, Turkey
[3]Ataturk University, Oltu Earth Sciences Faculty, Department of Geological Engineering, Erzurum, Turkey
[4]Department of Geothermics, Geology and Geophysics Institute, Baku, Azerbaijan

INFORMATION

Article history
Received 09 December 2019
Revised 26 December 2019
Accepted 26 December 2019
Available 31 December 2019

Keywords
Pillow lava
Back arc basin
Sevan-Akera-Qaradagh Ocean
Heiran
Ardabil

Contact
Yousef Vasigh*
yousefvasigh@yahoo.com

ABSTRACT

Heiran area is located in north-west of Ardabil and south west of Caspian Sea. Field evidences indicate submarine volcanic activities in this area. The rocks in this area are of basaltic composition. The outcrops of pillow lavas, prisms, dykes and lava flows in different points are evidences showing the existence of oceanic crust in this area. Studies on other locations of southern margin of Caspian Sea as well as structural and petrological similarities between Heiran and these areas may confirm the fact that Heiran area is part of geo-suture of Caspian Sea southern margin. The submarine lavas in this area are associated in age with late Cretaceous-Eocene. With regard to petrographical characteristics, the rocks under study range from andesitic basalt to olivine basalt and belong to alkaline series. The tectonomagmatic environment of these lavas is related to back arc basin. These magmas originate from subcontinental lithospheric mantle and have formed in a supra subduction environment. During upper Cretaceous-middle Paleogene, the closing of Sevan-Akera-Qaradagh Ocean led to the formation of marginal basin in the form of a back arc basin in the margin of Caspian Sea. The submarine lavas of Heiran area are likely to have originated from the volcanic activities of this marginal basin.

1. Introduction

Heiran area is located in north-west of Iran and south west of Caspian Sea (Fig. 1). Although the area has wonderful and exceptional vegetation, this prevents the outcrop of rocks from being easily observed. Outcrops from submarine basaltic lavas are seen in several locations in an area of 50 square kilometers. The oceanic crust of southern margin of Caspian Sea has long been a matter of argument. Annels et al. (1975) first introduced pillow lavas in the Qazvin-Rasht quadrangle map. Following this, similar lavas were studied in various areas including Chaloos, Lahijan, Amlash and Some'eh Sara. The rest of the submarine lavas continue to Heiran area. This study aims to introduce submarine basaltic lavas.

2. Field Study

The area under study is located 48˚, 31´ - 48˚, 37´ eastern longitude and 38˚, 23´ - 38˚, 26´ northern latitude. The outcrops of submarine lavas in the form of pillow lava, dyke, prism and lava flow are seen in different points of this area (Fig. 2). These lavas range in age between late Cretaceous to Eocene (Khodabandeh, 2001). The only sedimentary layer in this area is polygenic conglomerate which has outcropped locally and contains volcanic rocks and Jurassic and Cretaceous limestone. The formation of this conglomerate is associated to the lower Paleocene based on its microfossils which are Maastrichtian in age. These submarine lavas are located below and above the conglomerate. The formation of this conglomerate layer is likely to be the outcome of uplifting of basin floor in a local and island-like area.

Pillow lava is the most commonly observed structure in the region. These pillow lavas are 1-4 meters in size and are extended in shape (Fig. 3). They have circular or oval cross section in general but are seen in different shapes based on the topography of the place of extrusion and contact with other pillows. Basaltic prisms are the other structures which outcrop near the pillows. This adjacency indicates a relationship in origin between them. The basaltic prisms are seen below pillow lavas. The observable length of the prisms rarely exceeds 10 meters and is 35 centimeters, on average, in diameter. Also, the lava flows with basaltic composition have outcrops in some points. It is impossible to measure real thickness of these flows and their

observable thickness is less than 10 meters. The homogeneity of these masses likely indicates the cooling of the lava lake under the pillow lava. The structure of pillow lavas with lava lake is characteristic of a slow submarine eruption (Jutean and Maury, 1997). Unlike pillow lavas, these massive basalts are aphanitic and lack phenocrysts. The aphanitic texture of these basalts confirms their cooling in lava lake (Jutean et al., 1983).

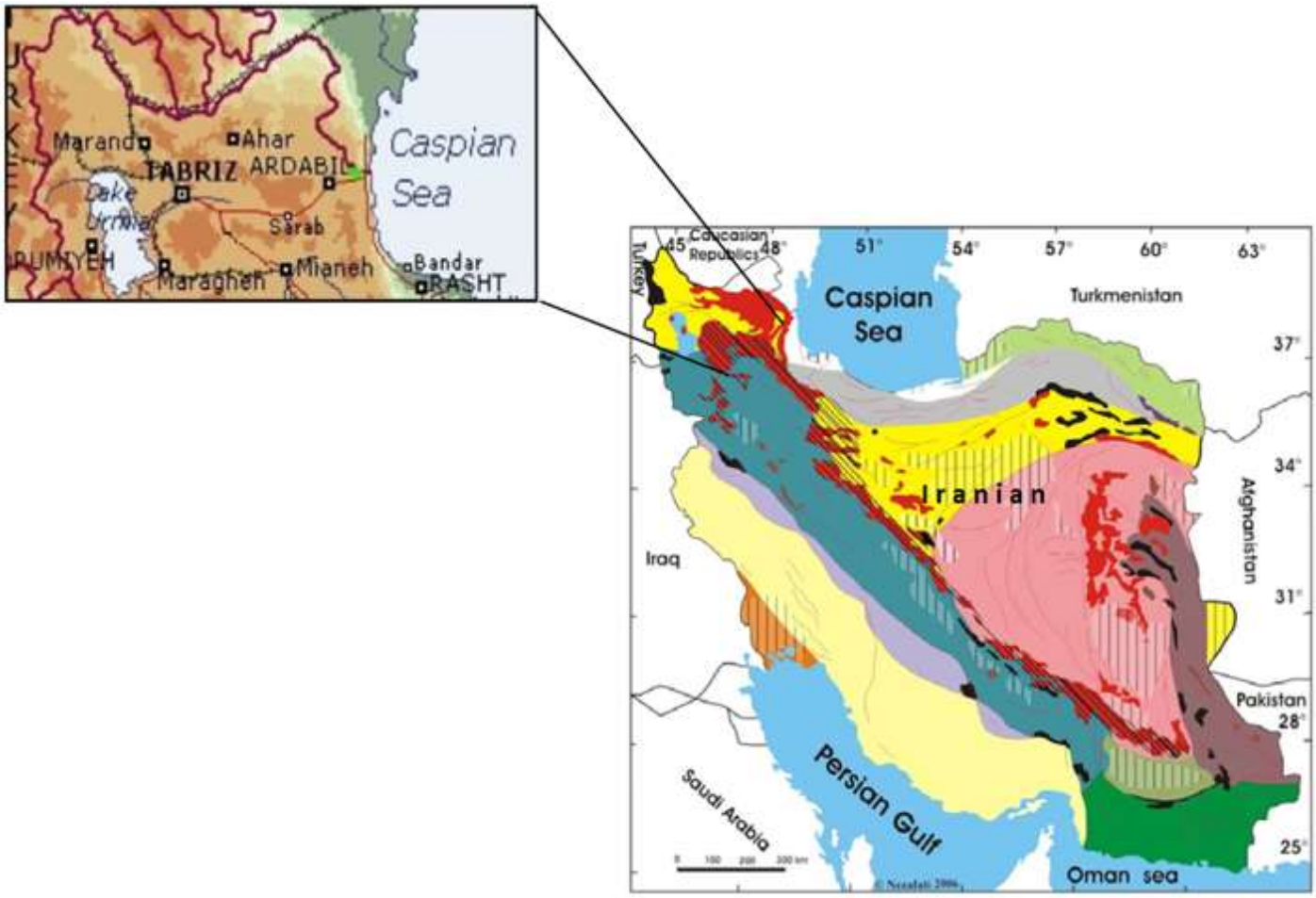

Fig. 1. Location map of study area (marked with green color)

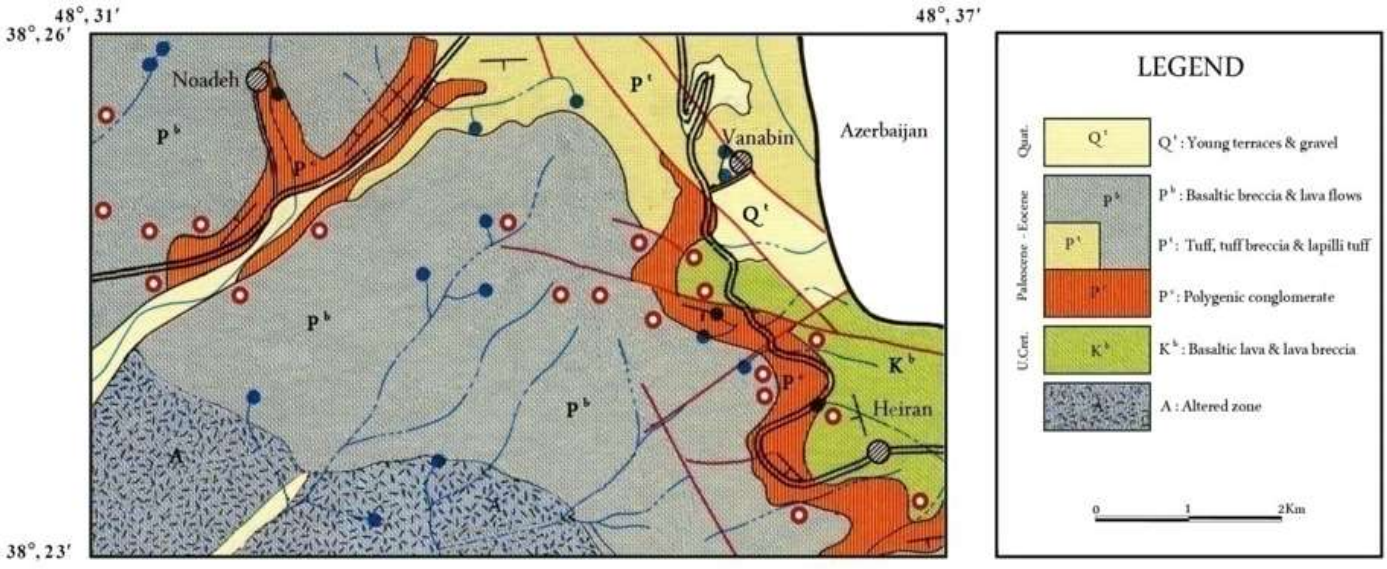

Fig. 2. Geological map of the under study area (red circles show outcrop of submarine lavas' location)

3. Petrography

The rocks under study are considered in a continuum ranging from andesitic basalt to olivine basalt. The texture of area rocks is porphyritic in general and is occasionally aphyric. As a result of accumulation of ferromagnesian minerals in some samples, there is also glomeroporphyritic texture (Fig. 4a). Matrix is usually microlitic and sometimes glassy microlitic. Based on their frequency, the fine minerals of matrix are as follows: plagioclase, pyroxene and opaque minerals.

Phenocrysts' ordering is as follows: clinopyroxene, plagioclase and olivine. Clinopyroxene phenocrysts are often automorphic, zoned and sector-zoned (Fig. 4b). Majority of plagioclase phenocrysts have labradorite-bytownite composition. Olivines are often sub automorphic and their roundness is indicative of nonequilibrium between olivine and matrix (Fig. 4c).

With respect to inclusion of the minerals, phenocrysts are crystallized in the following order: olivine, clinopyroxene and plagioclase. Acicular apatites have the largest amount among the minor minerals and are often inclusion (Fig. 4d).

Opaque minerals in different sizes are present in these rocks and are primary and secondary. These minerals are automorphic to xenomorphic. Some minerals such as calcite, quartz and zeolite with fluid phase have been formed in the rocks' porous and fissures.

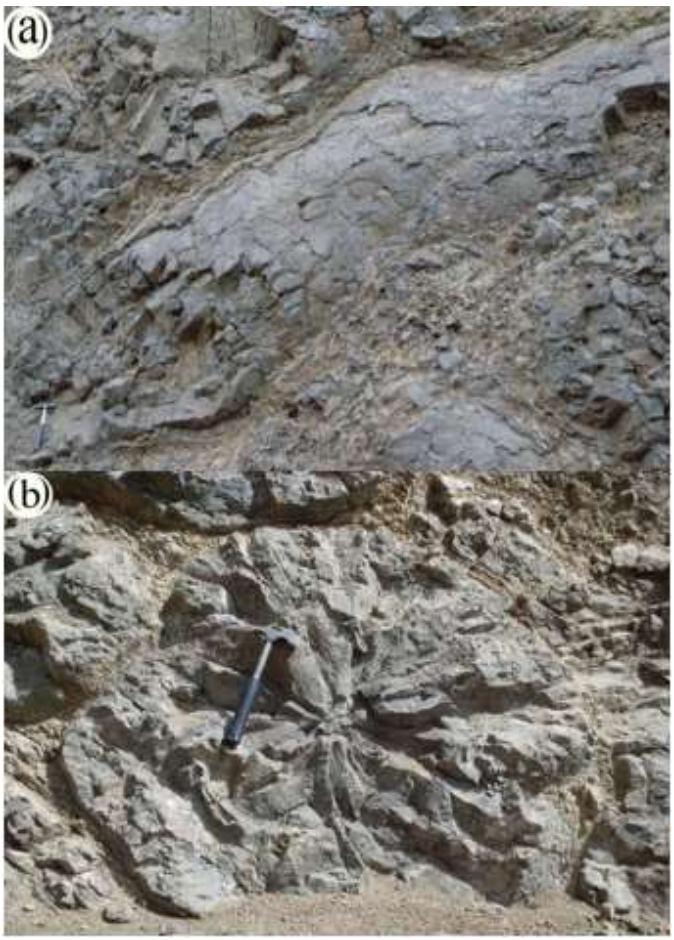

Fig. 3. (a) A sample of extended pillow lava with folded surface that shows the slop of basin floor during eruption, (b) Radial fracturing in core of the pillow lava due to cooling

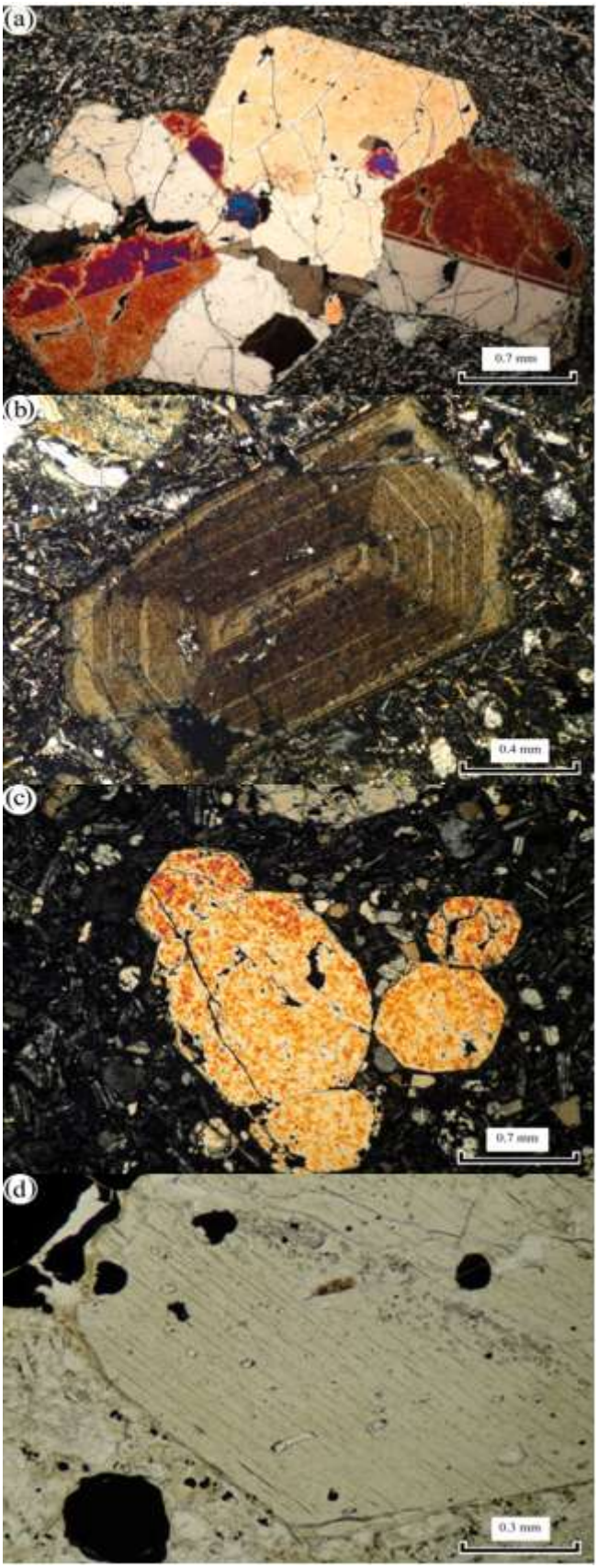

Fig. 4. (a) Glomeroporphyritic texture as a result of clinopyroxene accumulation with microlitic matrix in olivine basalt (XPL), (b) Clinopyroxene phenocryst in microlitic matrix that shows the zoning structure and sector-zone (XPL), (c) Rounded margins of the olivine phenocrysts due tononequilibrium with magma (XPL) and (d) Sections of apatites as a clinopyroxene inclusions (PPL)

4. Geochemistry

Twenty rock samples from the area were analyzed in SGS laboratory in Toronto using ICP-AES for 10 major oxides and ICP-MS for 40 rare elements (Tables 1 and 2). The rocks under study range from basalt, alkali basalt, alkali olivine basalt and hawaiite based on geochemical patterns. The magma of the area rocks has a certain association with alkaline series according to various patterns. Magmatic evolutions such as contamination, mixing, assimilation and differentiation change the preliminary composition of the magma toward sub alkaline series. The lack of linear trend in the geochemical diagrams is the result of these procedures. The rocks of the area are often rich in K and are in shoshonitic or at least high K series.

Table 1. Major element oxide analysis of the under study basalts

Oxide	H11	H17	H21	H22	H23	H25	H26	H27	H38	H39	H63	H66	H76	H77	H88	H91	H92	H93	H94	H95
SiO2	48.9	47.4	49.2	46.7	45.5	47.1	46.7	48.5	47.9	44.7	47	47.7	51.9	48.5	45.8	46.3	48.9	57.5	47.4	47.8
TiO2	0.83	1.11	0.88	0.87	1.15	0.84	1.06	0.87	0.89	0.77	1.04	1.11	0.96	1.04	0.76	0.54	1.07	0.51	0.95	1.08
Al2O3	20.1	16.9	13.3	14.3	16.9	19.2	15.4	12.8	16.7	11.7	15.5	16.3	16.7	15.2	11.7	18.2	17.7	20	16	18.3
Fe2O3	6.49	10	8.74	8.07	9.95	6.41	8.76	8.96	8.12	8.2	10	10.7	8.48	10.3	9.25	6.72	9.22	4.22	9.86	9.88
MnO	0.12	0.18	0.15	0.16	0.21	0.12	0.18	0.14	0.14	0.13	0.18	0.18	0.15	0.17	0.15	0.18	0.18	0.16	0.17	0.16
CaO	5.04	8.89	7.88	11.6	7.74	7.95	8.05	7.53	8.97	9.22	9.96	8.67	8.02	9.52	7.67	6.59	9.05	3.88	8.24	9.31
MgO	3.7	5.87	12.7	4.1	4.57	2.05	5.3	14.7	4.7	13	6.41	5.42	5.52	7.08	15.2	2.49	4.05	0.72	4.54	4.92
Na2O	3.4	4	2.2	2	5.3	2.4	2.8	1.9	2.7	1.4	2.8	4.1	2.7	2.2	2.8	8.4	3.4	5.5	4.8	3
K2O	5.38	1.72	2.64	5.05	1.38	4.44	5.25	2.25	3.42	2.35	1.85	1.83	2.59	2.16	1.56	0.38	2.43	6.16	1.74	2.2
P2O5	0.63	0.43	0.3	0.5	0.46	0.63	0.58	0.25	0.53	0.29	0.43	0.45	0.26	0.28	0.22	0.52	0.4	0.17	0.45	0.3

Table 2. Rare earth element concentrations (ppm) in the under study basalts

Sample	H11	H17	H21	H22	H23	H25	H26	H27	H38	H39	H63	H66	H76	H77	H88	H91	H92	H93	H94	H95
Ba	1010	500	430	1310	380	1000	720	360	750	380	590	700	410	430	370	870	650	770	1090	500
Ce	59.6	56.8	31.9	53.7	56.5	61.2	128	27.3	56.8	29.7	40.7	56.1	41.6	37.6	20.9	64	54.5	112	52	32.6
Co	15.3	32.5	46.1	26.5	29.2	16.7	26	50.2	27.4	45.3	32.4	31.6	27.5	37.4	56.3	21.3	23.7	5.2	29.5	31
Cr	68	68	821	68	68	68	68	821	205	889	137	68	205	205	1299	68	68	68	68	68
Cs	6	2.1	3.9	1.3	2.2	1.3	5	1.6	1.2	4.5	1.1	2.4	1.8	1.1	4.5	8.6	0.9	21.9	2	2.7
Dy	3.85	4.23	3.21	3.81	4.36	3.77	5.59	2.98	3.85	2.96	4.38	4.61	4.2	4.07	2.76	3.61	4.84	4.91	4.34	3.85
Eu	1.54	1.7	1.09	1.71	1.8	1.59	2.57	0.99	1.65	1.02	1.59	1.67	1.25	1.27	0.86	1.65	1.72	1.68	1.67	1.28
Gd	4.25	5.34	3.5	5.32	5.29	4.56	7.44	3.28	4.63	3.2	4.93	5.38	4.27	4.35	2.87	5.05	5.47	5.86	5.35	3.86
Hf	3	3	2	3	3	3	7	2	3	2	3	3	3	3	2	2	4	10	3	2
La	36.2	30.2	19.4	29.1	32.1	36.3	70.6	14.8	31.8	16.2	24.3	29.1	21.3	20.6	11.2	36	28.5	65.7	27.3	17.3
Lu	0.25	0.29	0.25	0.25	0.3	0.28	0.32	0.19	0.28	0.2	0.3	0.33	0.35	0.29	0.19	0.28	0.39	0.5	0.31	0.27
Nb	16	10	9	7	11	16	31	8	15	8	8	12	9	10	6	9	14	46	9	9
Nd	26.9	28.9	16.6	27.9	29.7	26.5	55.1	14.4	26.6	15.6	24.6	29.6	21	19.8	11.6	30.2	27.5	39.8	27.2	16.9
Ni	29	33	401	33	21	38	31	487	104	469	60	30	67	63	488	15	19	8	23	43
Pr	6.9	6.94	3.99	6.92	7.13	7.05	14.7	3.51	6.81	3.74	6.06	7.18	5.15	4.75	2.64	7.59	6.56	11.6	6.67	4.09
Rb	126	15.6	96	95.4	24.4	100	119	63.7	88.2	87	91.3	14.9	74.3	58.2	36.9	37.1	49	320	28.6	51
Sm	5.1	5.8	3.8	5.8	6.2	5.3	9.8	3.2	5.3	3.3	5.4	6.1	4.5	4.4	2.8	6.1	5.9	6.9	5.8	3.8
Sr	800	790	410	600	1050	3930	670	390	790	460	1060	950	450	450	360	280	790	1090	810	680
Ta	0.8	0.5	0.5	0.5	0.5	0.8	1.5	0.5	0.8	0.5	0.5	0.5	0.5	0.5	0.5	0.5	0.6	2.8	0.5	0.5
Th	8.4	6.2	4	6.3	5.9	8.8	21.6	3.3	8.7	3.5	3.3	5.9	5.6	3.8	2.4	11.7	5.9	40.6	6	3.3
U	1.86	1.62	1.05	2.42	1.63	2.44	6.6	0.95	3.6	1.06	0.83	1.59	1.43	0.87	0.49	4.02	1.65	12.6	1.29	0.91
Y	19.2	20.1	16.6	18.8	20.3	19.4	26.2	14.8	20.2	14.5	21.7	22.6	21.7	20.5	13.6	18.7	25	28.7	22.3	18.4
Yb	1.9	2	1.6	1.7	2	1.9	2.3	1.5	2	1.5	2.1	2.2	2.4	2.1	1.3	1.7	2.4	3.5	2.2	2
Zr	113	99	85.2	99.5	97.1	116	257	74.8	118	70.9	87.6	118	123	101	57.5	89.7	131	438	108	79.9

In spidergrams enrichments often comprise some LIL elements and depletions comprise some HFS elements (Fig. 5). In Sun et al. (1980) and Sun and McDonough (1989), spidergrams which are normalized with the primitive mantle and chondrite composition there is positive anomaly of K and Sr, and negative anomaly of Nb and Ti (Fig. 5c and d). In Pierce (1983) spidergram MORB normalized, there is positive anomaly of Th, Ba, Rb, K, Sm and Ce and negative anomaly of Nb, Ti and Zr (Fig. 5b). Positive anomaly of K is likely to be associated with magma source. Sr is a bivalent element and can replace Ca in plagioclases and create positive anomaly. Positive anomaly of Th, Ba and Ce can be related to contamination with crust. Accumulation of Ce in alkali basic rock seems to be reasonable (Smirnov et al. 1983). Apatite can also be a good container for Ce. Negative anomaly of Nb and Ti can be attributed to the contamination of magma with crust, fluid influences or differentiation crystallization. Also, the negative anomaly of Ti and Zr can be associated with partial crystallization of ilmenite and zircon. A comparison between basalt reference diagram (Pierce, 1983) (Fig. 5a) and spider gram of the samples indicated a similarity of the area rocks to continental margin basalts. The concentration of Ti, Nb, Ta and Th in these basalts is lower compared to its concentration within plate basalts.

According to different tectonomagmatic patterns such as Pearce and Gale (1977), Jenner et al. (1991) and Floyd et al. (1991), submarine lavas of the area are related to marginal basin and they show a specific relationship with volcanic arc environments especially with back arc basin (Fig. 6a, b and c). The chemistry of rocks confirms this. The volcanic rock of back arc basin is likely to be alkaline or sub alkaline (Gill, 1981). Gill (1981) and Wilson (1989) believe that LILE enrichments and relative HFSE depletion in the lavas of arc areas is common. One of the distinctive characteristics of the magmas of the volcanic arc environments is the proportion of Ba/Ta, which exceeds 450 in the arc magmas. In the samples under study this is 1096on average. The amount of TiO2 in arc area rocks hardly exceeds 1.3% (Gill, 1981). The amounts of this oxide in these samples are 0.5 to 1.15, which shows their relation to the arc environment.

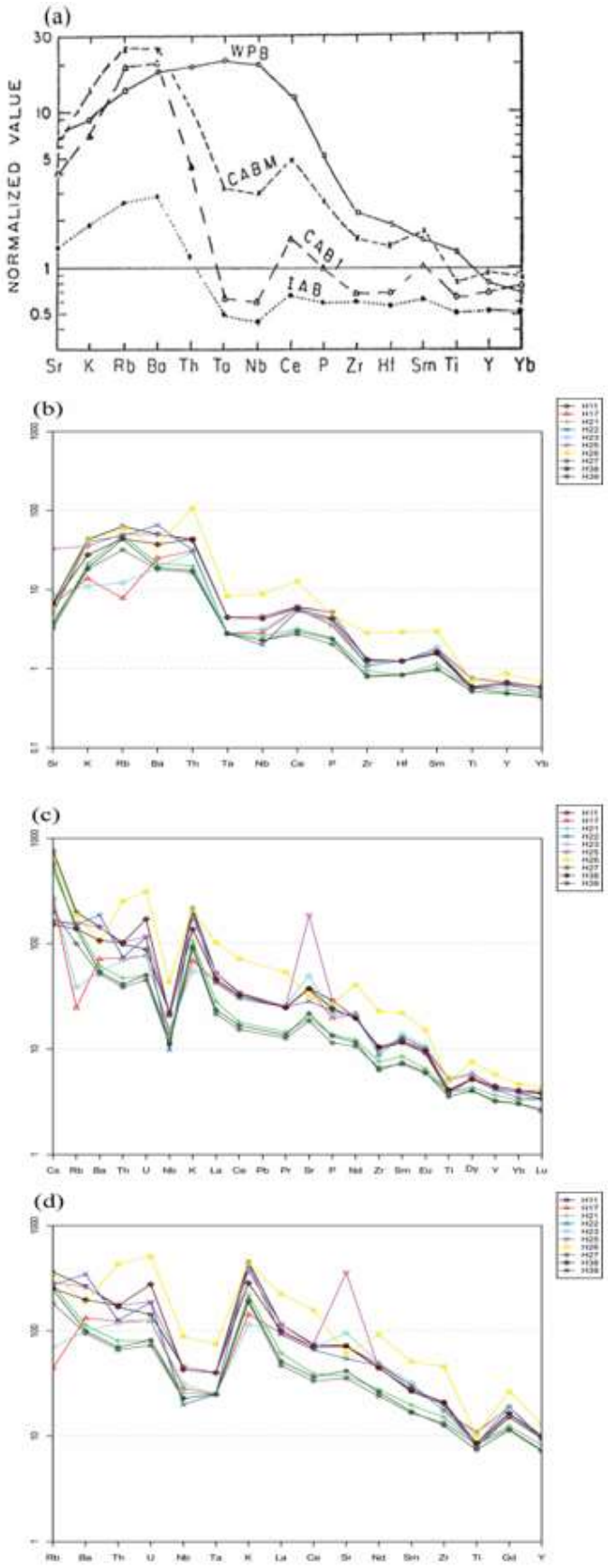

Fig. 5. (a) Pattern spidergram MORB normalized (Pearce, 1983), shows similarity of Heiran area basalts, (b) to marginal continental basalts (CABI), (c) Spidergram of primitive mantle normalized (after Sun and McDonough, 1989) and (d) Chondrite normalized (after Sun et al. 1980), showing positive K anomaly and negative Nb and Ta anomalies

According to different diagrams such as Ferrari et al. (2000) and Gil (1981), the study samples are related to subduction zone (Fig. 6d and e). The Ba/La ratio in the convergent plate margins is over 15 (Wood, 1980; Gill, 1981). This ratio is 23.2 on average for the area samples. The high ratio of Ba/La indicates the enrichment of mantle edge by subduction zone fluids and Ba can be created from subducted oceanic sediments (Wilson, 1989). The ratio of Sr/Nd is between 30-35 for the basalts of subduction zone (Hofmannet al., 1986). This ratio is 33.3 for the samples under study. The ratio of Nb/U for the MORB and OIB is approximately 47 whereas the value is lower for magmas associated with subduction environment (Hoffman et al. 1986). This is 7.2 on average for the area rocks, which is significantly different from MORB and OIB.

Based on Gill's (1981) classification the ratio of Ba/Nb in the subduction area rocks is above 30. With regard to basalts under study the value is 61.5 on average and is similar to the rocks of subduction zone. With regard to the spider diagrams, the negative anomalies of Zr, Ti, Nb and Ta and high ratio of LILE/HFSE and LREE/HREE show a similarity with the rocks of subduction area. The tectonomagmatic environment associated with back arc basin, chemical composition of area rock and their relationship with subduction process all indicate that area basalts have been formed in suprasubduction environment. The formation of alkaline rocks, in addition to tholeiitic rocks in the suprasubduction environments has been frequently reported in other studies (Nicoholson et al., 2000; Beccaluva et al., 2004; Bagci et al., 2006; Aldanmaz et al., 2008).

The original magma of the area rocks is related to lithospheric mantle. This is shown in several diagrams such as Hooper and Hawkesworth (1993) (Fig. 6f). Nowadays, it is proved that the great amount of deep crust and upper mantle rocks are particular to oceanic basins and some of the back arc basin (Jutean and Maury, 1997). These basalts form the crust of back arc basins or marginal basins that differ in wideness between 60 to over 1000 kilometers (Jutean and Maury, 1997).

Some HFS elements such as Nb lithospheric magma are various in amounts. Therefore, some scholars believe that La/Nb ratio can be affected by metasomatic enrichment (Abdel-Fattah et al., 2004). Bradshaw and Smith (1994) and Smith et al. (1999) showed that HFS elements such as Nb are depleted in lithospheric mantle compared to LRE elements such as La. As a result, the higher amount of Nb/La ratio (greater than 1) is indicative of asthenospheric mantle source and the lower amount of this ratio (less than 0.5) indicates a lithospheric mantle source. The average of this ratio in the area rocks is 0.41, which shows the lithospheric origin of the magma.

4.1. Microprobe study

Five samples of the area rocks were analyzed by electron microprobe in the laboratory of Hacettepe University in Ankara. Sixty-six points from clinopyroxene, plagioclase and olivine were analyzed.

Olivine: The microprobe analysis was conducted on 15 points of olivine. Regarding the amount of FeO and MgO, all samples have forsterite ($MgO_{91.1-94.5}$) composition except for one sample, which

is in chrysolite ($MgO_{79.1}$) array. This shows the high temperature of magma.

Clinopyroxene: 36 points of clinopyroxene were subjected to microprobe analysis, which according to wollastonite-enstatite-ferrosilite chemical system classification (Morimotoet al., 1988) reside in augite-diopside composition range.The amount was found to be (Wo_{45} En_{44} Fs_{11}) on average.

Plagioclase: Microprobe analysis was performed on 11 points of these minerals. According to orthoclase-albite-anorthite system classification (Deeret al., 1991) these samples are often of bytownite composition with inclination toward labradorite. These samples contain An_{63-87} and mostly placed in An_{75-79} and bytownite range.

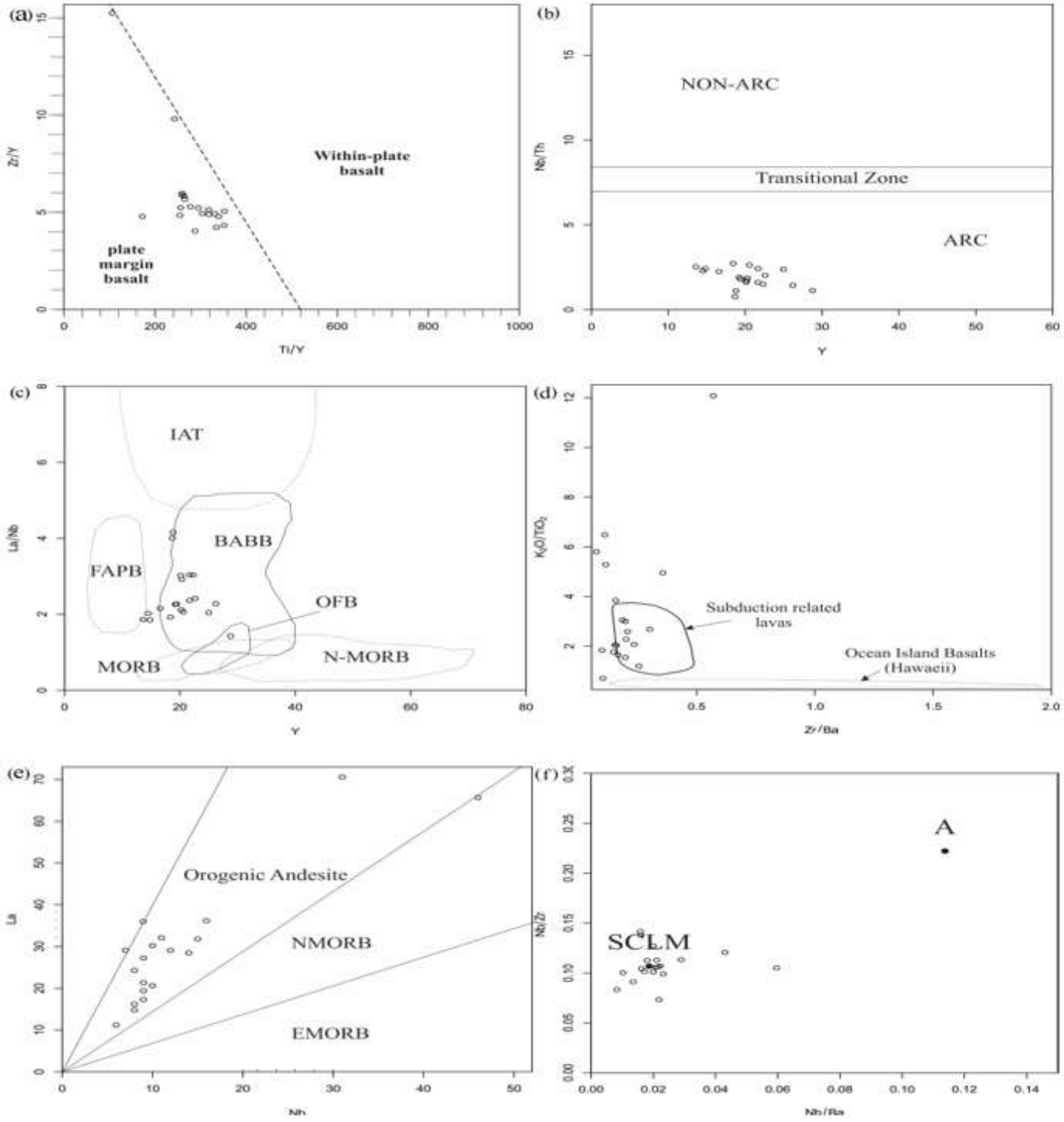

Fig. 6. Geochemical diagrams for determining composition and environment of rocks; (a) The plot of samples in the margin of plate in the Pearce and Gale (1977) pattern, (b) Diagram for separation of three environments of basalt formation (Jenner et al., 1991) in which the sample under study are in the arc environment array, (c) Plot of most of the samples in the back arc basin basalts array in the pattern for determining tectono magmatic environment of basalts (Floyd et al., 1991), (d) dependence of the area rocks on subduction environments in Ferrari et al. (2000)pattern, (e) the relation of most of the samples to orogenic environments in Gill (1981) classification, (f) the dependence of the area rocks magma on the subcontinental lithospheric mantle source (Hooper and Hawkesworth, 1993) (A: asthenospheric; SCLM: subcontinental lithospheric mantle)

4.2. Isotopic study

Four sample of the area rocks were analyzed using Sr-Nd (Rb-Sr and Sm-Nd) method in Carleton University, Ottawa (Table 3). The εNd ranges between -1.03 to 0.94 and is negative about three of the above mentioned samples, which shows enrichment by LREE and is probably indicating the process of contamination with continental crust during uprising of magma. Based on the isotopic diagram, $^{87}Sr/^{86}Sr$ versus $^{143}Nd/^{144}Nd$ (Zindler and Hart, 1986) the samples fall in the mantle array and are inclined toward Bulk Silicate Earth (BSE) (Fig. 7). The high ratios of $^{87}Sr/^{86}Sr$ in some samples, which has moved them away from mantle array, can be caused by the process of contamination with crust.

Table 3. Rb-Sr isotopic data of the basalts

Sample	$^{87}Sr/^{86}Sr$	$^{87}Rb/^{86}Sr$	$^{143}Nd/^{144}Nd$	$^{147}Sm/^{144}Nd$	εNd
H21	0.705984	0.677760	0.512585	0.13785	-1.03
H27	0.705569	0.472784	0.512615	0.13382	-0.45
H77	0.705331	0.374368	0.512594	0.13382	-0.86
H95	0.704628	0.217095	0.512686	0.13540	0.94

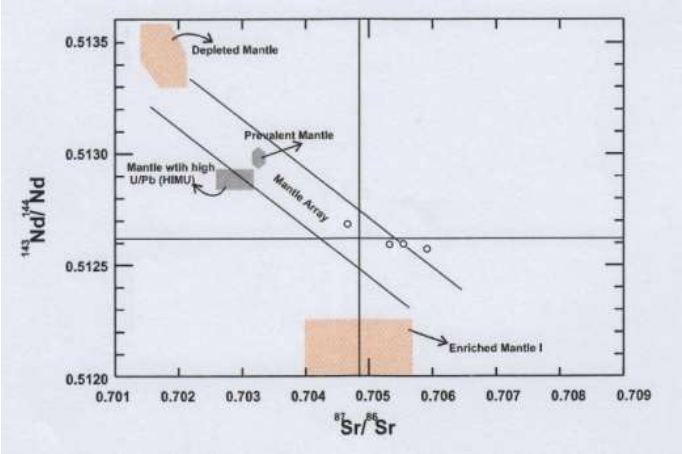

Fig.7. Situation of the area samples according to isotopic data (Zindler and Hart, 1986)

4.3. Geothermometry

The crystallization temperature has been computed using Helzand Thornber (1987) (I) and Putirka (2008) (II and III) equations. The equations I and II are based on the percentage of MgO in the ground mass and equation III is based on the percentage of FeO, Na_2O, K_2O and H_2O in the ground mass plus Mg#. The temperature variation range is 1275°c-1404°c and is 1349°c on average (Table 4). These equations and the results are listed below:

I. $T^{\circ c} = 20.1MgO^{liq} + 1014^{\circ c}$

II. $T^{\circ c} = 26.3MgO^{liq} + 994.4^{\circ c}$

III. $T^{\circ c} = 754 + 190.6(Mg\#) + 25.52(MgO^{liq}) + 9.585(FeO^{liq}) + 14.87(Na_2O + K_2O)^{liq} + 9.176(H_2O^{liq})$

Table 4. Thermometry results based on groundmass (whole rock) composition

Sample	T°c (1)	T°c (2)	T°c (3)	T°c (avg.)
H27	1309	1381	1386	**1359**
H39	1275	1336	1330	**1314**
H88	1320	1394	1404	**1373**

4.4. Geobarometry

Petrographic studies indicate that most of the clinopyroxenes show zoning. This is an indicator of rapid cooling and crystallization in lower pressures (Floweret al. 1977). Also, lack of homogeneity in chemical composition of clinopyroxenes and their zoning shows the rapid cooling as well as nonequilibrium (Burns, 1985; Parlak, 1996). Clinopyroxenes' Mg# is an effective measure of crystallization pressure of minerals. The primary clinopyroxenes which crystallize from a basaltic magma under lower pressure usually have Mg# lower than 84 (Groveand Bryan, 1983; Parlak et al., 2002). Clinopyroxenes of Hairan area have 68-74 Mg#. The lower value of Mg# in clinopyroxenes of the understudy area confirms their formation in lower pressure.

Nimisand Ulmer (1998) (I) and Putirka (2008) equations (II and III) were used to determine the crystallization pressure. Equation I is based on the value of cations present in the chemical composition of clinopyroxene and equations II and III are based on the chemical composition of clinopyroxene and coexisting melt as well as on the crystallization temperature. The variation in the crystallization pressure range between 3.8^{kb}-6.8^{kb}, 5.1^{kb} on average (Table 5). These equations and the results are listed below:

- $P^{kb} = 771.48 + 4.956(Al(\text{IV})) - 28.756(Fe) - 5.345(Fe^{3+}) + 56.904(Al(\text{VI})) + 1.848(Ti) + 14.827(Cr) - 773.74(Ca) - 736.57(Na) - 754.81(Mg) - 763.2(Fe) - 759.66(Mn) - 1.185(Mg)^2 - 1.876(Fe)^2$
- $P^{kb} = 3205 - 5.62(Mg) + 83.2(Na) + 68.2(DiHd) + 2.52\ln(Al(\text{VI})) - 51.1(DiHd)^2 + 34.8(EnFs)^2 + 0.384(T^k) - 518\ln(T^k)$
- $P^{kb} = 1458 + 0.197(T^k) - 241\ln(T^k) + 0.453(DiHd) + (DiHd) + 55.5(Al(\text{IV})) + 8.05(Fe) + 277(K) + 18(Jd) + 44.1\ 2.2\ln(Jd) - 27.7(Al)^2 + 97.3(Fe)^2 + 30.7(Mg)^2 - 27.6(DiHd)^2$

Table 5. Average of clinopyroxene crystallization pressure according to three methods

Sample	$P^{kb}(1)$	$P^{kb}(2)$	$P^{kb}(3)$	P^{kb} (avg.)
H27	3.9	6.3	4.2	**4.8**
H39	3.8	6.8	4.1	**4.9**
H88	4.5	6.3	5.7	**5.5**

5. Geodynamic

Subduction geochemical characteristics of the area rocks can be related to the closing of an ocean. Based on this fact, different researchers have referred to the existence of four oceans in the southern margin of the Caspian Sea.

Paleotethys Ocean: It has been closed during upper Paleozoic (Darvishzadeh, 1991). Taleshophiolites in southeast of the area are the only sign of this ocean in the southwest of Caspian Sea.

Second Paleotethys Ocean: It has started to form during the upper Paleozoic and early Mesozoic and simultaneous with the closing of Paleotethys Ocean. This ocean has been closed due to functioning of Indonesian orogenic phase in the early Cimmerian orogeny and simultaneous with the formation of Neotethys Ocean in southwest of Iran (Eftekharnejad et al., 1992).

IzAnCa (Izmir-Ankara-Caspian) Ocean: It has been formed along a line passing through north Turkey, Iran and central Afghanistan as a back arc basin during the subduction of

Neotethys Ocean. This ocean has been located in the east of Vardar Ocean passing through the southern margin of Caspian Sea and has been the back arc basin of Neotethys Ocean. This basin has been formed in Jurassic and has been close in early Cretaceous continuing until after Cretaceous (Stampfli and Borel, 2002; Cavazza et al., 2004).

Sevan-Akera-Qaradagh Ocean: The formation of which has been associated by Berberian (1983) with within-plate extension system. This process has given rise to the rifting between European plate (continental active margin of small Caucasian in the north) and central Iran (continental passive margin in southern Caucasian). Sevan-Akera-Qaradagh ocean has started to form in early Jurassic whose evidence have been reported in the outside borders of Iran and in the western parts of southern coast of Caspian Sea (Berberian, 1983). Adamia et al., (1977) and Knipper (1980) believe that the contact between north-western part of central Iran (Azerbaijan) and small Caucasian island arc during Cenomanian has started the closing of this ocean. Recent studies on the south of this geo-suture suggest a later time, namely Campanian-Maestrichtian (Berberian et al., 1981). Aghanabati (2004) believes that the contact movements related to the closing of Sevan-Akera-Qaradagh Ocean occurred in upper Cretaceous. The subduction of Sevan-Akera-Qaradagh oceanic crust has started with a north oriented slopeand has continued during Cretaceous (Adamia et al., 1977; Knipper, 1980; Berberian, 1983). In Campanian-Maastrichtian and at the same time when the Sevan-Akera-Qaradagh Ocean was being closed the marginal basin of southern Caspian Sea has been formed as a back arc basin on the Sevan-Akera-Qaradagh subduction (Salavati, 2008). Therefore, the closing of this geo-suture in different parts has taken place in different period of time with higher age for the closings of the east. Concerning geochemical characteristics and the age of submarine lavas of Heiran area, its association with Sevan-Akera-Qaradagh geo-suture seems to be logical so that the rocks of the area which show signs of formation above the subduction zone in the back arc basin have probably been formed somewhere in the back arc basin of Sevan-Akera-Qaradagh Ocean. On the other hand, the existence of alkaline rocks has been reported in different areas along the Sevan-Akera-Qaradagh geo-suture (Berberian, 1983; Dehghani and Makris, 1983; Salavati, 2008). Berberian (1983) believes that Eocene alkaline rocks of Azerbaijan and western Talesh as well as the alkaline basalt of northern Talesh in Azerbaijan Republic are the result of local faulting and rifting during the closing of Sevan-Akera-Qaradagh Ocean.

6. Conclusion

Submarine lavas of Heiran area has been formed above a convergent zone with an extension in late Cretaceous and early Tertiary. Results of geothermometery, geobarometery and Mg# of clinopyroxenes show high temperature and low pressure during the formation of rocks, which confirm the extensional environment. Some geochemical features in these rocks such as enrichment with LREE and LILE and depletion from HFSE indicate the effect of subduction parameters and consequently the formation of these lavas in correspondence with the subduction zone in the back arc basin. This is quite similar to the formation of ophiolites corresponding to supra-subduction environments. These lavas have probably originated in lithospheric mantle as a result of the effect of fluids emanating from subducted plate and have been contaminated with crust during the rising procedure. The transitional alkaline lavas in the marginal ocean along the southern Caspian Sea, which are likely to be Sevan-Akera-Qaradagh back arc basin, have formed submarine structure in late Cretaceous-Eocene and have probably been overthrusted in late Paleocene on the northern Alborz as a result of the complete closure of this ocean.

References

Abdel-Fattah, M., Abdel-Rahman, A. M., Nassar, P.E., 2004. Cenozoic Volcanism in the Middle East: Petrogenesis of alkali basalts from northern Lebanon. Geol. Mag. 141 (5), 545-563.

Adamia, Sh. A., Lordkipanidze, M.B., Zakariadze, G.S., 1977. Evolution of an active continental margin as exemplified by the Alpine history of the Caucasus. Tectonophysics, 40 (3/4), 183-199.

Aghanabati, A., 2004. Geology of Iran, Geological Survey of Iran, 586p.

Aldanmaz, E., Yaliniz, M.K., Guctekin, A., Goncuoglu, M.C., 2008. Geochemical characteristics of mafic lavas from the Neotethyanophiolites in western Turkey: implications for heterogeneous source contribution during variable stages of ocean crust generation. Geol. Mag. 145 (1), 37-54.

Annels, R.N., Arthurton, R.S., Basley, R.A., Davies, R.G., 1975. Explanatory text of Qazvin-Rasht quadrangles map, 1:250000, Geological Survey of Iran.

Bagci, U., Parlak, O., Hock, V., 2006. Geochemical character and tectonic environment of Ultramafic to mafic cumulate rocks from the Tekirova (Antalya) ophiolites (southern Turkey). Geological Journal 41, 193-219.

Beccaluva, L., Coltortia, M., Giuntab, G., Siena, F., 2004. Tethyan vs. Cordilleran ophiolites: a reappraisal of distinctive tectono-magmatic features of supra-subduction complexes in relation to the subduction mode. Tectonophysics 393, 163-174.

Berberian, M., 1983. The southern Caspian: A compression floored by a trapped modified oceanic crust. Canadian Earth Science 20, 163-183.

Berberian, M., Babakhani, A.R., Amidi, M., 1981. Exploration of southern protraction of Sevan-Akera-Qaradagh geo-suture, internal report, Geological Survey of Iran.

Bradshaw, T.K., Smith, E.I., 1994. Polygenetic Quaternary volcanism at Crater Flat, Nevada. Journal of Volcanology and Geothermal Research 63, 165-182.

Burns, L.E., 1985. The Border Ranges ultramafic and mafic complex, south-central Alaska: Cumulate fractionates of island arc volcanics. Canadian Journal of Earth Sciences 22, 1029-1038.

Cavazza, W., Roure, F.M., Spakman, W., Stampfli, G.M., Ziegler, P.A., 2004. The TRAVSMED atlas, the Mediterranean region from crust to mantle, Verlag Berlin Heidelberg, 141.

Darvishzadeh, A., 1991. Geology of Iran, Amir Kabir publication, 901.

Deer, W.A., Howie, R.A., Zussman, J., 1991. An introduction to the rock forming minerals, Longman Scientific and Technical, 528.

Dehghani, G.A., Makris, J., 1983. The gravity field and structure of Iran, In Geodynamic Project (Geotraverse) in Iran. G. S. Report No. 51, 51-68.

Eftekharnezhad, J., Asadian, A., Mirzaei, A.R., 1992. Age of Shanderman-Asalem metamorphic and ophiolitic complex and relationship with Paleotethys and sub oceanic crust of Caspian Sea. Geosciences 3, 4-15.

Ferrari, L., Conticelli, S., Vaggelli, G., Petrone, Ch., Manetti, P., 2000. Late Miocene volcanism and intra-arc tectonics during the early development of Trans-Mexican Volcanic Belt. Tectonophysics 318, 161-185.

Flower, M.F.J., Robinson, P.T., Schmincke, H.U., Ohnmacht, W., 1977. Magma fractionation systems beneath the Mid Atlantic ridge at 36-37jN. Contribution Mineralogy and Petrology 64, 167-195.

Floyd, P.A., Kelling, G., Gokcen, S.L., Gokcen, N., 1991. Geochemistry and tectonic environment of basaltic rocks from the Miss ophiolitic mélange, south Turkey. Chemical Geology 89, 263-280.

Gill, J.B., 1981. Orogenic andesites and plate tectonics. Springer, Berlin, 489.

Grove, T.L., Bryan, W.B., 1983. Fractionation of pyroxene-phyric MORB at low pressure: an experimental study. Contributions to Mineralogy and Petrology Journal of Geology 84, 293-309.

Hart, W. K., WoldeGabrie, G., Walter, R.C., Mertzman, S.A., 1989. Basaltic volcanism in Ethiopia: constraints on continental rifting and mantle interactions. Journal of Geophysical Research 94, 7731-7748.

Helz, R.T., Thornber, C.R., 1987. Geothermometery of Kilauea Ikilava lake, Hawaii. Bulletin of Volcanology 49, 651-668.

Hofmann, A.W., Jochum, K.P., Seufert, M., White, W.M., 1986. Nb and Pb in ocean basalts: new constraints on mantle evolution. Earth and Planetary Science Letters 79, 33-45.

Hooper, P.R., Hawkesworth, C.J., 1993. Isotopic and geochemical constraints on the origin and evolution of the Colombia River Basalts. Journal of Petrology 34, 1203-1264.

Jenner, G.A., Dunning, G.R., Malpas, J., Brown, M., Brace, T., 1991. Bay of Islands and Little Port complexes, revisted age, geochemical and isotopic evidence confirm suprasubduction zone origin. Canadian Journal of Earth Sciences 28, 1635-1652.

Jutean, T., Erssen, J.P., Monin, A.S., Zonenshin, L.P., Sorokhtin, O.G., Matveenkov, V.V., Almukhamedov, A.I., 1983. Structure et petrologie du rift axial de la Mer Rouge vers 18 N, Bull. Cent. Rech. Explor. Prod. Elf Aquitatine 7, 217-231.

Jutean, T., Maury, R., 1997. Geologie de la croute oceanique petrologei et dynamique endogens. Masson, 569.

Khodabandeh, A.A., 2001. Explanatory text of Astara quadrangles map, 1:100000, Geological survey of Iran.

Knipper, A., 1980. The tectonic position of ophiolites of Lesser Caucasus. In Ophiolites.Edited by A. Panayiotou.Proceedings, International ophiolite Symposium. Geology Survey Department, Ministry of Agriculture and National Resources, Cyprus, 372-376.

Morimoto, N., Fabries, J., Ferguson, A.K., Ginzburg, I.V., Ross, M., Seifert, F.A., Zussman, J., Gottardi, G., 1988. Nomenclature of pyroxenes. Mineralogy and Petrology 39, 55-76.

Nicoholson, K.N., Black, P.M., Picard, C., 2000. Geochemistry and tectonic significance of the Tangihua Ophiolite Complex, New Zealand. Tectonophysics 321, 1-15.

Nimis, P., Ulmer, P., 1998. Clinopyroxene geobarometry of magmatic rocks, Part 1: an expended structural geobarometer for anhydrous and hydrous basic and ultrabasic systems, Contrib. Mineralogy and Petrology 133, 122-135.

Parlak, O., 1996. Geochemistry and geochronology of the Mersin ophiolite within the eastern Mediterranean tectonic frame (Southern Turkey), Theses doctorate. Universite de Genève, Terre and Environment, 242.

Parlak, O., Hock, V., Delaloye, M., 2002. The supra-subduction zone Pozanti-Kars antiophiolite, Southern Turkey: evidence for high-pressure crystal fractionation of Ultramafic cumulates. Lithos 65, 205-224.

Pearce, J.A., 1983. Role of the sub-continental lithosphere in magma genesis at active continental margins: Hawkesworth C. J., and Norry, M. J. (eds), Continental basalts and mantel xenoliths, Shiva, Nantwich, 230-249.

Pearce, J.A., Gale, G.H., 1977. Identification of ore-deposition environment from trace element geochemistry of associated igneous host rocks. Geological Society Special Publications 7, 14-24.

Putirka, K.D., 2008. Thermometers and barometers for volcanic systems. Reviews in Mineralogy and Geochemistry 69, 61-120.

Salavati, M., 2008. Petrology and Geochemistry of ophiolitic complex from the East Gilan, PhD Thesis, Sciences Faculty, University of Esfahan, 241.

Smirnov, V.I., Gnizburg, A.I., Grigoriev, Y.M., Yakolove, G.F. 1983. Studies of mineral deposits, Mir Publishers, Moscow, 288.

Smith, E.I., Sanchez, A., Walker, J.D., Wang, K., 1999. Geochemistry of mafic magmas in the hurricane Volcanic Field, Utah: implications for small and large scale chemical variability of the lithospheric mantle. Journal of Geology 107, 433-448.

Stampfli, G.M., Borel, G.D., 2002. A plate tectonic model for the Paleozoic and Mesozoic constrained by dynamic plate boundaries and restored synthetic ocean isochrones. Earth and Planetary Science Letters 196, 17-33.

Sun, S.S., Bailey, D.K., Tarney, J., Dunham, K., 1980. Lead isotopic study of young volcanic rocks from mid-ocean ridges, ocean islands and island arcs. Philos Trans. R. Soc. London, A297, 409-445.

Sun, S.S., McDonogh, W.F., 1989. Chemical and isotopic systematic of ocean basalts: implication for mantle composition and processes. In: Saunders A. D. and Norry M.J.(Eds.) Magmatism in Ocean Basins, Geological Society of London Special Publication, 313-345.

Wilson, M., 1989. Igneous petrogenesis. Unwin Hyman London. 466.

Wood, D.A., 1980. The application of a Th-Hf-Ta diagram to problems of tectonomagmatic classification and to establishing the nature of crustal contamination of basaltic lavas of the British Tertiary volcanic province. Earth and Planetary Science Letters, 50, 11-30.

Zindler, A., Hart, S.R., 1986. Chemical geodynamics. Annual Review of Earth and Planetary Science 14, 493-571.